Cell Reports
Article

RIP3 Inhibits Inflammatory Hepatocarcinogenesis but Promotes Cholestasis by Controlling Caspase-8- and JNK-Dependent Compensatory Cell Proliferation

Mihael Vucur,[1,11] Florian Reisinger,[5,11] Jérémie Gautheron,[1,2,11] Joern Janssen,[1] Christoph Roderburg,[1] David Vargas Cardenas,[1] Karina Kreggenwinkel,[1] Christiane Koppe,[1] Linda Hammerich,[1] Razq Hakem,[7] Kristian Unger,[6] Achim Weber,[8] Nikolaus Gassler,[3] Mark Luedde,[9] Norbert Frey,[9] Ulf Peter Neumann,[4] Frank Tacke,[1] Christian Trautwein,[1] Mathias Heikenwalder,[5,10] and Tom Luedde[1,*]

[1]Department of Medicine III
[2]Interdisciplinary Centre for Clinical Research (IZKF)
[3]Institute of Pathology
[4]Department of Visceral and Transplantation Surgery
University Hospital RWTH Aachen, D-52074 Aachen, Germany
[5]Institute of Virology, Helmholtz Zentrum München für Gesundheit und Umwelt (HMGU), D-81675 Munich, Germany
[6]Research Unit of Radiation Cytogenetics, Helmholtz-Zentrum München für Gesundheit und Umwelt (HMGU), D-85764 Neuherberg, Germany
[7]Departments of Medical Biophysics and Immunology, Ontario Cancer Institute, University of Toronto, Toronto, ON M5G 2C1, Canada
[8]Institute of Surgical Pathology, University Hospital Zurich, CH-8091 Zurich, Switzerland
[9]Department of Cardiology and Angiology, University Hospital Kiel, D-24105 Kiel, Germany
[10]Institute of Virology, Technische Universität München (TUM), D-81675 Munich, Germany
[11]These authors contributed equally to this work
*Correspondence: tluedde@ukaachen.de
http://dx.doi.org/10.1016/j.celrep.2013.07.035

SUMMARY

For years, the term "apoptosis" was used synonymously with programmed cell death. However, it was recently discovered that receptor interacting protein 3 (RIP3)-dependent "necroptosis" represents an alternative programmed cell death pathway activated in many inflamed tissues. Here, we show in a genetic model of chronic hepatic inflammation that activation of RIP3 limits immune responses and compensatory proliferation of liver parenchymal cells (LPC) by inhibiting Caspase-8-dependent activation of Jun-(N)-terminal kinase in LPC and non-parenchymal liver cells. In this way, RIP3 inhibits intrahepatic tumor growth and impedes the Caspase-8-dependent establishment of specific chromosomal aberrations that mediate resistance to tumor-necrosis-factor-induced apoptosis and underlie hepatocarcinogenesis. Moreover, RIP3 promotes the development of jaundice and cholestasis, because its activation suppresses compensatory proliferation of cholangiocytes and hepatic stem cells. These findings demonstrate a function of RIP3 in regulating carcinogenesis and cholestasis. Controlling RIP3 or Caspase-8 might represent a chemopreventive or therapeutic strategy against hepatocellular carcinoma and biliary disease.

INTRODUCTION

Hepatocellular carcinoma (HCC), the most common primary liver tumor, arises almost exclusively in a setting of chronic hepatic inflammation (Sherman, 2010). However, the knowledge on the clear association between inflammation and cancer has not yet translated into a chemopreventive pharmacological strategy against HCC development, underlining the need for a better understanding of molecular processes controlling the transition from inflammation to cancer. Cell death represents a dominant trigger for inflammation, thus contributing to multiple hallmark capabilities of cancer (Hanahan and Weinberg, 2011). In chronic liver disease, hepatocyte cell death is a prominent feature driving progression to hepatic fibrosis and finally HCC (Zhang and Friedman, 2012).

For years, the term apoptosis was used synonymously for programmed cell death, whereas necrosis was considered a passive, not specifically regulated, and ATP-independent process (Chakraborty et al., 2012). Apoptosis is triggered by ligation of death receptors, like tumor necrosis factor (TNF) receptor, by their cognate ligands and represents a highly synchronized procedure depending on activation of aspartate-specific proteases, known as caspases (Chakraborty et al., 2012). In viral hepatitis, immune cell-triggered apoptosis of virally infected hepatocytes represents a key step in viral clearance (Fung et al., 2009). Moreover, apoptotic death of hepatocytes is a common feature of alcoholic and nonalcoholic steatohepatitis and is associated with fibrosis (Feldstein and Gores, 2005).

It was recently discovered that, next to apoptosis, necroptosis—programmed necrosis depending on the kinases receptor interacting protein 1 (RIP1) and RIP3—represents an alternative programmed cell-death pathway downstream of the TNF-receptor (Cho et al., 2009; He et al., 2009; Zhang et al., 2009). It can be induced by viral infection and can serve as an alternative when caspase-dependent apoptosis is inhibited or absent (Han et al., 2011). Necroptosis plays a role in the regulation of chronic inflammation in the pancreas, gut, and skin (Bonnet et al., 2011; He et al., 2009; Welz et al., 2011). In human patients, necroptosis is activated in alcoholic liver injury (Roychowdhury et al., 2013) as one of the leading causes of liver cirrhosis and HCC in the western world (Sherman, 2010). However, the functional role of RIP3 in controlling the consequences of chronic inflammation in the liver and other organs is presently not known. In this study, we examined the role of RIP3 in a model of inflammatory hepatocarcinogenesis based on conditional deletion of the mitogen-activated protein 3 (MAP3)-kinase transforming growth factor β (TGF-β)-activated-kinase-1 (TAK1) in liver parenchymal cells (LPC) (TAK1$^{LPC\text{-}KO}$) (Bettermann et al., 2010).

RESULTS

RIP3 Is Activated in TAK1-Deficient Livers and Promotes Jaundice and Cholestasis by Inhibiting a Sufficient Ductular Reaction

Mice with conditional deletion of *Tak1* in LPC (TAK1$^{LPC\text{-}KO}$ mice) display severe hepatic inflammation at a young age characterized by spontaneous LPC apoptosis and LPC necrosis, proceeding over time to liver fibrosis and liver cancer but also to severe lethal cholestasis (Bettermann et al., 2010). In order to investigate the function of RIP3 in hepatocarcinogenesis, we generated mice with ablation of TAK1 in LPC together with a full knockout of *Rip3* (TAK1$^{LPC\text{-}KO}$/RIP3$^{-/-}$) or combined ablations of TAK1 and Caspase-8 in LPC (TAK1/Casp-8$^{LPC\text{-}KO}$) and first compared their phenotypes with wild-type (WT) and TAK1 single mutant mice (TAK1$^{LPC\text{-}KO}$) at the age of 6 weeks (Figure 1A).

We detected strongly increased protein levels of RIP3 in liver extracts from TAK1$^{LPC\text{-}KO}$ and TAK1/Casp-8$^{LPC\text{-}KO}$ mice (Figure 1A), suggesting that LPC in these mice might be sensitized to necrosis (He et al., 2009). Measurements of serum enzymes from 6-week-old male mice confirmed that TAK1$^{LPC\text{-}KO}$ mice showed a strong rise in serum aminotransferases (alanine aminotransferase [ALT] and aspartate aminotransferase [AST]) and serum glutamate dehydrogenase (GLDH) levels compared to WT mice as marker for hepatitis and LPC damage (Figure 1B). Macroscopic analysis revealed that this coincided with yellow color of livers and elevated serum bilirubin and alkaline phosphatase (AP) levels (Figures 1B and 1C), reflecting severe jaundice and cholestasis as shown previously by electron-microscopical analysis of bile canaliculi in TAK1$^{LPC\text{-}KO}$ animals (Bettermann et al., 2010). Moreover, TAK1$^{LPC\text{-}KO}$ livers displayed macroscopically visible nodules on the surface of livers (Figure 1C). Deletion of *Caspase-8* in TAK1$^{LPC\text{-}KO}$ mice led to significant reduction in ALT, AST, and GLDH serum levels, and disappearance of macroscopic nodules on the surface of liver lobes compared to TAK1$^{LPC\text{-}KO}$ mice. However, no rescue in hyperbilirubinemia and AP elevation was found (Figures 1B and 1C). In contrast, deletion of *Rip3* in TAK1$^{LPC\text{-}KO}$ mice led to a normalization of bilirubin and reduced AP levels but worsened hepatitis, indicated by significantly elevated ALT and GLDH levels in TAK1$^{LPC\text{-}KO}$/RIP3$^{-/-}$ mice compared to TAK1$^{LPC\text{-}KO}$ animals (Figure 1B). Moreover, while at 6 weeks of age, TAK1$^{LPC\text{-}KO}$/RIP3$^{-/-}$ livers lacked a yellow color as a sign of jaundice; they displayed multiple small nodules on their surface (Figure 1C).

Histological analysis of liver sections from 6-week-old male mice revealed that jaundice in TAK1$^{LPC\text{-}KO}$ mice correlated with the presence of areas of hepatocyte necrosis, which were detected even to a higher extent in TAK1/Casp-8$^{LPC\text{-}KO}$ animals, whereas necrosis was absent in TAK1$^{LPC\text{-}KO}$/RIP3$^{-/-}$ mice at this age (Figures 2A and 2B). In parallel to the absence of necrosis, TAK1$^{LPC\text{-}KO}$/RIP3$^{-/-}$ mice showed a strong ductular reaction with expansion of A6^{+} (oval) cells (Figures 2A–2D), likely reflecting a necessary process to maintain biliary homeostasis in a setting of chronic inflammation (Desmet, 2011; Glaser et al., 2009). Strikingly, this ductular reaction was absent in TAK1$^{LPC\text{-}KO}$ and TAK1/Casp-8$^{LPC\text{-}KO}$ mice (Figures 2A, 2C, and 2D). These data demonstrate that, in chronic hepatitis, Caspase-8-dependent apoptosis primarily causes elevation of free circulating aminotransferases and GLDH in the serum. In contrast, RIP3-dependent necroptosis promotes jaundice and cholestasis in TAK1$^{LPC\text{-}KO}$ livers, because it is not linked with a ductular reaction.

Activation of RIP3 Limits Compensatory Proliferation of Hepatocytes and Biliary Epithelial Cells in the Chronically Inflamed Liver

We further analyzed the influence of RIP3 and Caspase-8 on cell death in TAK1$^{LPC\text{-}KO}$ animals. In line with previous findings (Bettermann et al., 2010), TAK1$^{LPC\text{-}KO}$ mice displayed significant spontaneous LPC apoptosis as shown by immunohistochemistry and western blot analyses for cleaved Caspase-3 (Figures 3A–3C). Additional deletion of *Caspase-8* resulted in complete inhibition of Caspase-3 cleavage, whereas additional deletion of *Rip3* in TAK1$^{LPC\text{-}KO}$ mice resulted in a significant increase in Caspase-3 cleavage when compared to TAK1$^{LPC\text{-}KO}$ mice (Figures 3A–3C). Therefore, Caspase-8-dependent apoptosis and RIP3-dependent necroptosis counterbalance and compete with each other in the regulation of LPC death in TAK1$^{LPC\text{-}KO}$ livers (compare Figures 2A and 2B and Figures 3A–3C).

We next examined the functions of Caspase-8 and RIP3 in LPC proliferation in *Tak1*-deficient livers. Ki67 staining and western blot analyses of the cell cycle proteins proliferating cell nuclear antigen (PCNA) and cyclin D1 confirmed a high proportion of proliferating LPC in TAK1$^{LPC\text{-}KO}$ mice (Figures 3A–3C). Additional deletion of *Caspase-8* dramatically reduced the number of proliferating LPC and the degree of PCNA/cyclin D1 expression, whereas proliferation remained high or was even higher by tendency in mice with combined deletions of *Tak1* and *Rip3* (Figures 3A–3C). This indicates that Caspase-8-dependent LPC apoptosis induces strong compensatory proliferation of other adjacent LPC, which is not the case in terms of LPC necroptosis. Interestingly, not only hepatocytes but also biliary cells in TAK1$^{LPC\text{-}KO}$/RIP3$^{-/-}$ mice displayed increased apoptosis and proliferation, as indicated by costainings for pancytokeratin and Ki67 or cleaved Caspase-3 (Figures 3D–3F). Thus, differential degrees of compensatory cell proliferation

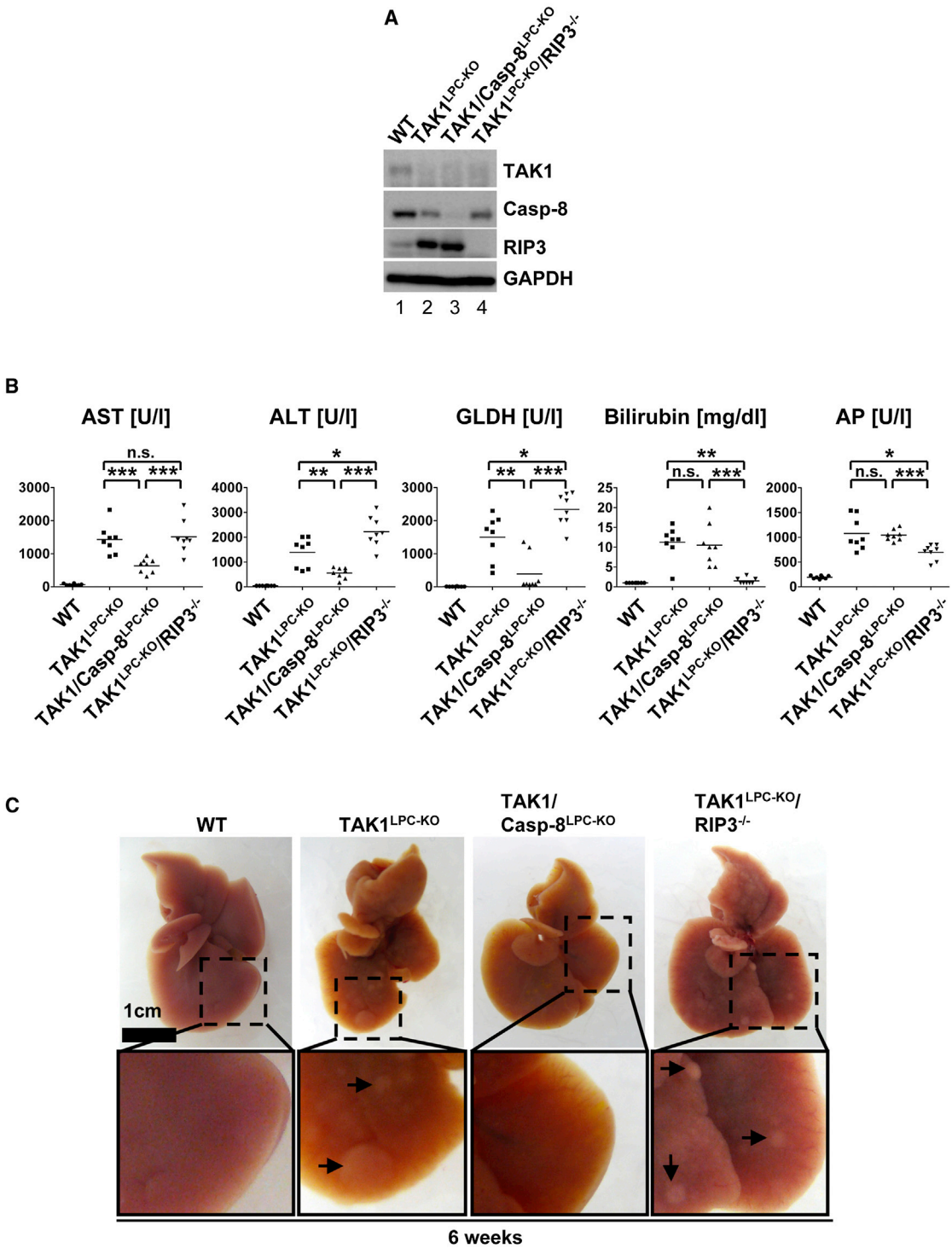

Figure 1. Apoptosis and Necroptosis Differentially Regulate Dysplasia, Cholestasis, and Liver Injury in Mice with LPC-specific *Tak1* Deletion

(A) Western blot analysis of whole liver protein extracts from 6-week-old male TAK1^{LPC-KO}, TAK1/Casp-8^{LPC-KO}, TAK1^{LPC-KO}/RIP3$^{-/-}$, and control littermate mice (WT) using antibodies against TAK1, RIP3, Caspase-8, and glyceraldehyde 3-phosphate dehydrogenase (GAPDH) as loading control.

(B) Serum level analysis of AST, ALT, glutamate dehydrogenase (GLDH), total bilirubin, and AP in 6-week-old male mice. Results are shown as mean. Double asterisks denote $p < 0.01$ and triple asterisks denote $p < 0.001$ ($n = 8$ each genotype).

(C) Representative macroscopic pictures of 6-week-old male WT, TAK1^{LPC-KO}, TAK1/Casp-8^{LPC-KO}, and TAK1^{LPC-KO}/RIP3$^{-/-}$ livers. Small nodular structures are observed in livers of TAK1^{LPC-KO} and TAK1^{LPC-KO}/RIP3$^{-/-}$ mice but not on TAK1/Casp-8^{LPC-KO} livers. Arrows indicate nodules. Additionally, TAK1^{LPC-KO} and TAK1/Casp-8^{LPC-KO} but not TAK1^{LPC-KO}/RIP3$^{-/-}$ livers display a cholestatic, yellow color. The scale bars represent 1 cm.

upon apoptosis versus necroptosis are a likely cause for the presence or absence of a sufficient ductular reaction and cholestasis in TAK1$^{LPC\text{-}KO}$/RIP3$^{-/-}$ and TAK1/Casp-8$^{LPC\text{-}KO}$ mice, respectively.

To evaluate the effect of *Caspase-8* deletion in LPC, we further performed serological and histological analyses on Casp-8$^{LPC\text{-}KO}$ mice. This analysis revealed mild liver injury, indicated by elevated serum ALT, AST, and GLDH, but no changes in the biliary system or infiltration with myelomonocytic cells (Figures S1A–S1C). In addition, we tested whether the molecules Caspase-8 or RIP3 might have limiting effects on LPC proliferation and performed partial hepatectomy (PH) experiments in Casp-8$^{LPC\text{-}KO}$ mice or mice with constitutive deletion of *Rip3* (RIP3$^{-/-}$). Whereas WT and RIP3$^{-/-}$ animals showed similar expression levels of cell cycle markers cyclin D1 and PCNA in western blot and Ki67-expression in immunohistochemical analysis, Casp-8$^{LPC\text{-}KO}$ animals even displayed a slight acceleration in cell-cycle progression (Figures S1D–S1F). This indicates that the differences in the proliferative response between TAK1$^{LPC\text{-}KO}$/RIP3$^{-/-}$ and TAK1/Casp-8$^{LPC\text{-}KO}$ animals were not caused by direct effects of Caspase-8 or RIP3 on the cell-cycle machinery, however, suggest that apoptosis but not necroptosis of LPC represents a strong trigger for compensatory LPC proliferation.

The kinase TAK1 integrates signals from several upstream ligands and regulates various inflammatory and stress-related signaling pathways (Delaney and Mlodzik, 2006). We therefore tested whether, besides apoptosis and necroptosis, other signaling pathways might be involved in hepatitis and cholestasis development in *Tak1*-deficient livers and generated mice with combined deletions of *Tak1* and *Caspase-8* in LPC together with full knockout of *Rip3* (TAK1/Casp-8$^{LPC\text{-}KO}$/RIP3$^{-/-}$ mice; Figure S2A). On macroscopic, serological, and histological level, combined deletions of *Caspase-8* and *Rip3* completely rescued hepatitis, liver injury, cholestasis, and biliary ductopenia seen in TAK1 single mutants (Figures S2B–S2D). This highlights that apoptosis and necroptosis represent the major pathways mediating the severe phenotype in *Tak1*-deficient livers. Further, this argues against significant influences of potential dysregulation of biliary transporters or structural cell proteins in biliary epithelial cells in response to *Tak1* deletion.

Activation of RIP3 Inhibits Hepatic Tumor Growth

Based on the differential functional relations between apoptotic versus necroptotic cell death and compensatory LPC proliferation, we next evaluated if RIP3 and Caspase-8 might also differentially regulate hepatocarcinogenesis. Hence, we examined the spontaneous phenotype of 25- to 38-week-old animals, because TAK1 single mutants develop HCC at that age (Bettermann et al., 2010). Macroscopic analyses of livers confirmed the presence of hepatic tumors in TAK1$^{LPC\text{-}KO}$ mice (Figure 4A). Surprisingly, TAK1/Casp-8$^{LPC\text{-}KO}$ animals did not show any signs of macroscopically detectable hepatic tumors at this age. In contrast, TAK1$^{LPC\text{-}KO}$/RIP3$^{-/-}$ mice exhibited a massive hepatic tumor burden already visible on macroscopic level (Figure 4A). The high hepatic tumor burden in these mice corresponded with a significant increase in the liver-to-body weight ratio in TAK1$^{LPC\text{-}KO}$/RIP3$^{-/-}$ animals compared to TAK1 single mutants or TAK1/Casp-8 combined mutants (Figure 4B). On the histological level, we confirmed increased development of hepatic tumors with histological criteria of HCC in TAK1$^{LPC\text{-}KO}$/RIP3$^{-/-}$ mice by hematoxylin and eosin staining (H&E) staining and immunohistochemical analysis for collagen-IV expression. Conversely, no histologically malignant hepatic tumor or preneoplastic lesions could be detected in TAK1/Casp-8$^{LPC\text{-}KO}$ animals (Figures 4C and 4D). Thus, Caspase-8-dependent apoptosis promotes HCC development in TAK1$^{LPC\text{-}KO}$ mice. In contrast, the higher tumor burden in TAK1$^{LPC\text{-}KO}$/RIP3$^{-/-}$ mice compared to TAK1$^{LPC\text{-}KO}$ mice and the absence of hepatic tumors in TAK1/Casp-8$^{LPC\text{-}KO}$ livers exhibiting pure necroptosis suggest that activation of RIP3 has an inhibitory effect on tumor growth. Importantly, the fact that the massive tumor development in TAK1$^{LPC\text{-}KO}$/RIP3$^{-/-}$ mice could be completely abolished by cell-specific ablation of *Caspase-8* in LPC (TAK1/Casp-8$^{LPC\text{-}KO}$/RIP3$^{-/-}$ mice) (Figures S2E and S2F) argues against a significant effect of *Rip3* deletion in nonparenchymal hepatic cells in the regulation of hepatocarcinogenesis in TAK1$^{LPC\text{-}KO}$/RIP3$^{-/-}$ mice, which have an LPC-specific knockout of *Tak1* but full knockout of *Rip3*.

The finding that TAK1/Casp-8$^{LPC\text{-}KO}$ mice did not develop any HCC, whereas TAK1$^{LPC\text{-}KO}$/RIP3$^{-/-}$ mice showed larger HCC than TAK1$^{LPC\text{-}KO}$ single mutant animals, suggested that activation of RIP3 controls hepatocarcinogenesis in terms of the hepatic tumor burden. To test if RIP3 also influences hepatic tumor biology, HCC samples from TAK1$^{LPC\text{-}KO}$ and TAK1$^{LPC\text{-}KO}$/RIP3$^{-/-}$ mice were profiled by qRT-PCR with a 16 gene signature that identifies and stratifies liver tumors according to their degree of differentiation and proliferation rate (Cairo et al., 2008). For control, normal liver samples as well as samples of aggressive liver tumors from woodchuck hepatitis virus (WHV)/N-myc2 p53^{+}/delta mice (Renard et al., 2000) were added to the analysis. Unsupervised analysis of the samples profiled showed coclustering of nearly all TAK1$^{LPC\text{-}KO}$ and TAK1$^{LPC\text{-}KO}$/RIP3$^{-/-}$ tumors (Figure 4E). We also examined expression of alpha fetoprotein (AFP) and selected oncogenes and tumor suppressor genes (antigen-presenting cell [APC], p53, E2F transcription factor 5 [E2F5], cyclin-dependent kinase inhibitor 2A [CDKN2A], cyclin D1, neuroepithelial cell transforming 1 [Net1], FgR, and Jun) in HCC from both mouse lines. Despite elevated cyclin D1 and APC levels in TAK1$^{LPC\text{-}KO}$/RIP3$^{-/-}$ tumors, most other genes examined showed similar transcriptional levels in HCC from TAK1$^{LPC\text{-}KO}$ and TAK1$^{LPC\text{-}KO}$/RIP3$^{-/-}$ livers (Figure 4F). Together, these findings indicate similar tumor biology of HCC in both mouse lines, suggesting that activation of RIP3 in TAK1$^{LPC\text{-}KO}$ mice inhibits hepatocarcinogenesis by a dominant effect on tumor initiation and proliferation of tumor cells.

RIP3 Controls the Transition from Inflammation to Cancer by Inhibiting Caspase-8-Induced Chromosomal Aberrations Associated with Immortalization of Hepatocytes

To further analyze the functional roles of necroptosis and apoptosis on hepatocarcinogenesis, we performed array-comparative genomic hybridization (aCGH) analyses on histologically characterized and microdissected HCCs from TAK1$^{LPC\text{-}KO}$

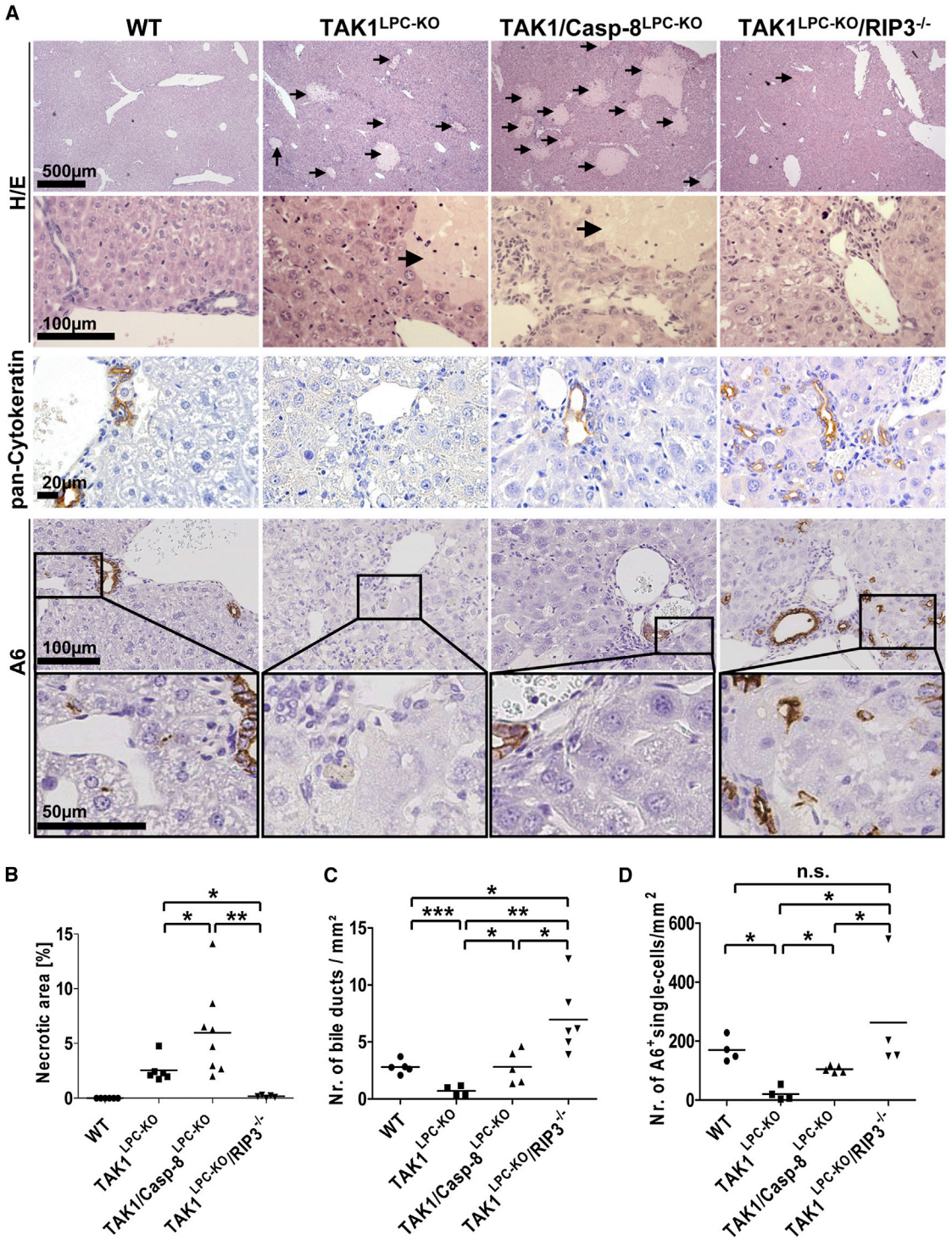

Figure 2. RIP3-Dependent Necroptosis Mediates Cholestasis and Biliary Ductopenia by Suppressing Caspase-8-Dependent Ductular Reaction in Livers of Mice with LPC-Specific *Tak1* Deletion

(A) Histological (H&E) and immunohistochemical (pancytokeratin, A6) analysis on representative liver sections from 6-week-old male mice. Arrows indicate necrotic areas. The scale bars represent (from top to bottom) 500 μm, 100 μm, 20 μm, 100 μm, and 50 μm.

(B) Evaluation of necrotic areas from H&E staining. WT (n = 6), TAK1^{LPC-KO} (n = 6), TAK1/Casp-8^{LPC-KO} (n = 6), and TAK1^{LPC-KO}/RIP3$^{-/-}$ (n = 5) livers. Results are shown as mean. The asterisk denotes $p < 0.05$ and double asterisks denote $p < 0.01$.

(legend continued on next page)

and TAK1$^{LPC\text{-}KO}$/RIP3$^{-/-}$ mice and areas of disturbed microarchitecture (histologically not HCC or dysplastic nodules) in TAK1/Casp-8$^{LPC\text{-}KO}$ animals (Figure 5A). As previously shown for TAK1$^{LPC\text{-}KO}$ mice (Bettermann et al., 2010) and corroborated on three HCCs in this study, TAK1$^{LPC\text{-}KO}$ displays large chromosomal amplifications mainly on chromosomes 4, 8, and 13. Interestingly, amplifications on these chromosomes were also found in most tumors of TAK1$^{LPC\text{-}KO}$/RIP3$^{-/-}$ mice. However, the majority of TAK1$^{LPC\text{-}KO}$/RIP3$^{-/-}$ tumors displayed multiple additional chromosomal aberrations, of which many were not found in tumors of most TAK1$^{LPC\text{-}KO}$ animals (chromosomes 1, 5–6, 9, and 11–12; Figure 5A; Bettermann et al., 2010). In contrast, TAK1/Casp-8$^{LPC\text{-}KO}$ animals hardly displayed any significant chromosomal aberrations in their livers (Figure 5A). These data suggest that, in chronic hepatitis, apoptosis but not necroptosis specifically promotes the development of liver cancer by favoring an environment that drives genetic aberrations. Moreover, necroptosis not only inhibits tumor growth but also counterbalances the establishment of genetic alterations in HCC.

The striking pattern of chromosomal aberrations detected in TAK1$^{LPC\text{-}KO}$ and TAK1$^{LPC\text{-}KO}$/RIP3$^{-/-}$ tumors but not livers of TAK1/Casp-8$^{LPC\text{-}KO}$ mice prompted us to further investigate if these genetic changes might withhold a functional role in the transition from inflammation to cancer (e.g., by driving LPC specifically resistant to apoptotic cell death). To test this, we isolated primary hepatocytes from 8-week-old WT, TAK1/Casp-8$^{LPC\text{-}KO}$, and TAK1$^{LPC\text{-}KO}$/RIP3$^{-/-}$ mice, lacking immunohistochemical and molecular evidence for malignant tumors (data not shown). Twenty-four hours after isolation, cells were washed carefully to remove dead cells and then stimulated with recombinant murine TNF, a treatment that induces cell-death of *Tak1*-deficient but not WT hepatocytes, due to their inability to activate nuclear factor (NF)-κB (Bettermann et al., 2010). Twenty-four hours after TNF stimulation, TAK1/Casp-8$^{LPC\text{-}KO}$ but not WT hepatocytes lost attachment to the plate and showed morphological signs of cell death (Figure 5B), indicating that TNF treatment led to necroptosis of hepatocytes in vitro. Whereas also many hepatocytes isolated from TAK1$^{LPC\text{-}KO}$/RIP3$^{-/-}$ livers showed morphological signs of cell death, some cells with large nuclei survived TNF treatment and were collected for preparation of genomic DNA followed by aCGH analysis for their genetic status. Strikingly, cells displayed the same pattern of chromosomal aberrations on chromosomes 4, 8, and 13 as seen previously in HCC from these animals as well as additional chromosomal aberrations (Figure 5C). These data provide evidence that the specific, Caspase-8-dependent pattern of chromosomal aberrations on chromosomes 4, 8, and 13 in TAK1$^{LPC\text{-}KO}$/RIP3$^{-/-}$ mice arises already at an early step of hepatocarcinogenesis and is associated with immortalization of hepatocytes in a setting of Caspase-8-dependent apoptosis. In line with this hypothesis, we identified focal areas free of Caspase-3 activation already in 6-week-old TAK1$^{LPC\text{-}KO}$/RIP3$^{-/-}$ mice (Figure S3), probably reflecting in vivo a corresponding early step of clonal immortalization.

Caspase-8-Dependent Apoptosis but Not RIP3-Dependent Necroptosis Is Associated with a Strong Inflammatory Response and Liver Fibrosis

We aimed at further characterizing mediators of compensatory LPC proliferation activated in response to Caspase-8 but not RIP3-dependent necroptosis. Liver regeneration was previously shown to involve the production of inflammatory cytokines secreted by hepatic macrophages/Kupffer cells (Michalopoulos and DeFrances, 2005), suggesting that differential inflammatory responses to LPC apoptosis versus necroptosis might be associated with the differences in LPC proliferation between both respective mouse lines. Fluorescence-activated cell sorting (FACS) analysis revealed stronger infiltration of myeloid cells and CD4$^+$ and CD8$^+$ T cells but similar levels of B cells in both TAK1$^{LPC\text{-}KO}$ and TAK1$^{LPC\text{-}KO}$/RIP3$^{-/-}$ mice compared with WT and TAK1/Casp-8$^{LPC\text{-}KO}$ animals (Figure 6A; data not shown). Immunohistochemical analysis confirmed a clear trend toward higher numbers of F4/80$^+$ cells in TAK1$^{LPC\text{-}KO}$/RIP3$^{-/-}$ mice compared with TAK1/Casp-8$^{LPC\text{-}KO}$ animals (Figure 6B). To further examine expression levels of cytokines typically secreted by activated macrophages, we performed a FACS-based microbeads fluorescence assay on liver homogenates, which revealed significantly higher protein levels of interleukin (IL)-1α, IL-6, and IL-10 in TAK1$^{LPC\text{-}KO}$ and TAK1$^{LPC\text{-}KO}$/RIP3$^{-/-}$ compared to TAK1/Casp-8$^{LPC\text{-}KO}$ animals (Figure 6C), of which IL-1α and IL-6 represent key cytokines driving compensatory proliferation and HCC development in response to hepatocyte death (Maeda et al., 2005; Sakurai et al., 2008). Thus, in contrast to previous concepts of oncotic necrosis versus necrosis (Jaeschke and Lemasters, 2003), we show here that LPC apoptosis rather than necroptosis drives inflammation in response to chronic injury.

We further tested for the presence of liver fibrosis by Sirius red stainings on liver slides from 6-week-old WT, TAK1/Casp-8$^{LPC\text{-}KO}$, and TAK1$^{LPC\text{-}KO}$/RIP3$^{-/-}$ mice. This analysis showed only a slight increase in fibrosis in TAK1/Casp-8$^{LPC\text{-}KO}$ livers at that age, which in turn was significantly lower than seen in TAK1$^{LPC\text{-}KO}$/RIP3$^{-/-}$ animals (Figure S4A). Additional RT-PCR analysis on whole liver RNA extracts revealed only a trend toward higher levels of TGF-β1 and TGF-β3 in TAK1$^{LPC\text{-}KO}$/RIP3$^{-/-}$ mice compared with TAK1/Casp-8$^{LPC\text{-}KO}$ livers (Figure S4B). Whereas levels of active TGF-β ligands might not be fully reflected on RNA levels, due to potential differences in cleavage processes (Dubois et al., 2001), these data suggest that apoptosis but not necroptosis induces hepatic fibrogenesis and activation of stellate cells by various profibrogenic and proinflammatory stimuli.

(C) Statistical quantification of number of bile ducts per mm^2 in WT (n = 5), TAK1$^{LPC\text{-}KO}$ (n = 4), TAK1/Casp-8$^{LPC\text{-}KO}$ (n = 5), and TAK1$^{LPC\text{-}KO}$/RIP3$^{-/-}$ (n = 6) livers. TAK1$^{LPC\text{-}KO}$ livers show decreasing of bile ducts, whereas, in TAK1$^{LPC\text{-}KO}$/RIP3$^{-/-}$, livers increase the number of bile ducts compared with the other genotypes. Results are shown as mean. The asterisk denotes $p < 0.05$, double asterisks denote $p < 0.01$, and triple asterisks denote $p < 0.001$.
(D) Statistical analysis of A6$^+$ single-oval cells per mm^2 in the respective 6-week-old mice. Results are shown as mean (n = 4, except for TAK1/Casp-8$^{LPC\text{-}KO}$ mice, where n = 5); *$p < 0.05$; n.s., not significant.

Cell PRESS
Open ACCESS

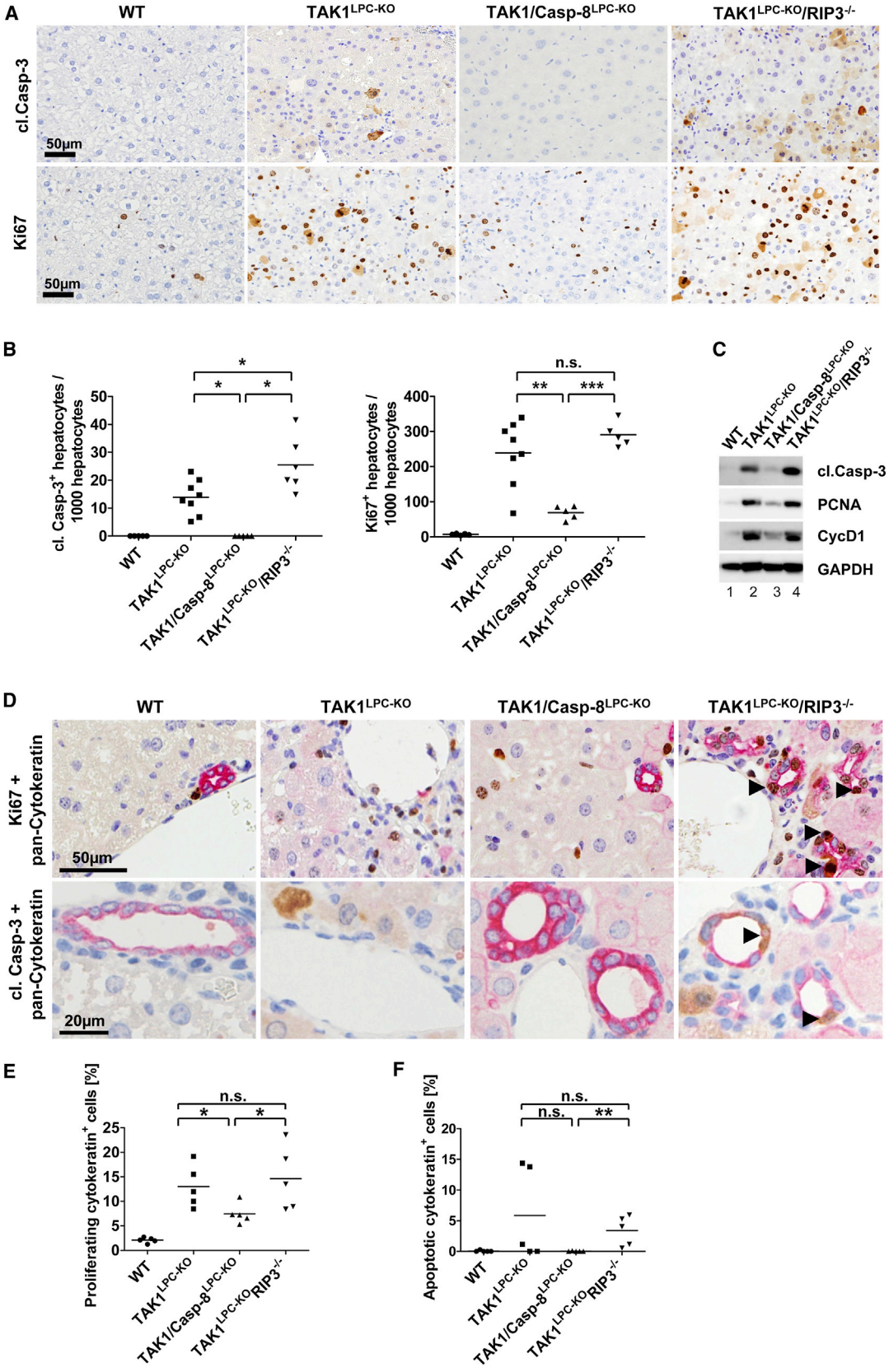

(legend on next page)

Caspase-8-Dependent Apoptosis Drives Compensatory LPC Proliferation by Activation of JNK in Parenchymal and Nonparenchymal Liver Cells

We further examined which intracellular signaling pathways might connect the two different modes of cell death with activation or inhibition of compensatory proliferation and cancer development. In *Drosophila*, activation of Jun-(N)-terminal kinase (JNK) by the initiator caspase Dronc is driving apoptosis-induced compensatory proliferation (Huh et al., 2004; Kondo et al., 2006). Moreover, it was suggested that JNK activation is part of a nonapoptotic, procarcinogenic pathway downstream of CD95/Fas/APO-1 (Chen et al., 2010). Western blot analysis on liver extracts from 6-week-old mice revealed strong spontaneous phosphorylation and activation of JNK but not p38α, AKT, or ERK in livers of TAK1$^{LPC\text{-}KO}$/RIP3$^{-/-}$ compared with TAK1/Casp-8$^{LPC\text{-}KO}$ and WT animals (Figure 7A). Immunohistochemical staining for the phosphorylated JNK forms confirmed significantly more phosphorylated JNK (p-JNK)$^{+}$ hepatocytes in TAK1$^{LPC\text{-}KO}$/RIP3$^{-/-}$ compared to TAK1/Casp-8$^{LPC\text{-}KO}$ and WT animals (Figure 7B). Importantly, TAK1$^{LPC\text{-}KO}$/RIP3$^{-/-}$ livers even displayed significantly more p-JNK^{+} hepatocytes than TAK1$^{LPC\text{-}KO}$ single knockouts (Figure 7C). In addition, TAK1$^{LPC\text{-}KO}$/RIP3$^{-/-}$ livers showed a significantly higher fraction of p-JNK^{+} liver nonparenchymal cells (NPC) than all other genotypes, although to a much lower extent than observed in terms of hepatocytes (Figure S5). Finally, to functionally evaluate the role of JNK in mediating apoptosis and compensatory proliferation in TAK1$^{LPC\text{-}KO}$/RIP3$^{-/-}$ mice, we injected TAK1$^{LPC\text{-}KO}$/RIP3$^{-/-}$ mice with the well-established JNK-inhibitor SP600125, which significantly decreased the amount of Ki67^{+} cells and lowered cyclin D1 expression when compared to vehicle-treated animals (Figures 7D, 7E, and 7G). Additional analysis of cleaved Casp-3^{+} cells lacked a significant difference between the two groups (Figures 7D and 7F). These data suggest that JNK activation represents an important step in mediating compensatory proliferation downstream of Caspase-8, whereas, in contrast, RIP3 inhibits the activation of JNK in livers of TAK1$^{LPC\text{-}KO}$ mice.

DISCUSSION

The natural course of chronic hepatic disease is characterized by a relatively uniform pattern, featuring constant hepatocyte cell death, inflammation and compensatory hepatocyte proliferation, hepatic fibrogenesis, and ultimately the development of HCC (Sherman, 2010). Although this sequence has been known for many years, it has not been well characterized which exact molecular pathways are regulating the critical transition from inflammation to cancer, which explains why, up to now, no nonpathogen-specific chemopreventive strategy has been developed against HCC in patients with chronic liver disease. We show that, in a setting of chronic inflammation induced by LPC-specific deletion of *Tak1*, RIP3-dependent necroptosis represents a pathway regulating the consequences of chronic inflammation in the liver by counteracting against Caspase-8-dependent compensatory proliferation of hepatocytes, immune cell activation, hepatic fibrogenesis, and the development of chromosomal aberrations leading to hepatocarcinogenesis.

Studies have demonstrated that necroptosis serves as an alternative when caspase-dependent apoptosis is inhibited or absent (Han et al., 2011). Of note, our findings indicated the simultaneous activation of both apoptosis and necroptosis in livers of TAK1$^{LPC\text{-}KO}$ animals, mediating either carcinogenesis or cholestasis. *Tak1* deletion in LPC results in inhibition of NF-κB activation (Bettermann et al., 2010), which in turn leads to increased sensitivity against spontaneous apoptosis, as demonstrated in mice with conditional deletion of the NF-κB-activating kinase subunit NF-κB essential modulator (NEMO) (Luedde et al., 2007; Wunderlich et al., 2008). On the other hand, it was recently shown in vitro that TAK1 can prevent necroptosis by inhibiting the action of RIP1/RIP3 complexes (Vanlangenakker et al., 2011), supporting the hypothesis that TAK1 inhibits activation of both programmed cell death pathways in LPC. Based on our findings, it is likely that, in the absence of *Rip3*, LPC are "forced" to die by apoptosis, leading to increased inflammation and a higher tumor burden in TAK1$^{LPC\text{-}KO}$/RIP3$^{-/-}$ mice. TAK1 is therefore a master regulator of liver cell death induced, for example, by the cytokines TNF-α and TGF-β (Inokuchi et al., 2010; Yang et al., 2013). Moreover, the fact that cultured primary TAK1-deficient hepatocytes show a decreased survival in serum-free conditions (Bettermann et al., 2010) indicates also an intrinsic component of cell death in these cells.

As stated before, livers with conditional deletion of *Tak1* in LPC show defective NF-κB activation and—similar to other mouse models with genetic defects in the NF-κB pathway

Figure 3. Apoptosis but Not Necroptosis Induces Strong Compensatory Proliferation of Hepatocytes and Biliary Epithelial Cells upon Chronic Liver Injury

(A) Immunohistochemical analysis on representative liver paraffin sections from 6-week-old male mice of the indicated genotypes. Upper panel: cleaved (cl.) Caspase-3 staining. Lower panel: Ki67 staining. The scale bars represent 50 μm.

(B) Statistical analysis of Ki67^{+} and cl. Casp-3^{+} hepatocytes. Results are shown as mean (cl. Casp-3 staining: WT [n = 5]; TAK1$^{LPC\text{-}KO}$ [n = 8]; TAK1/Casp-8$^{LPC\text{-}KO}$ [n = 5]; TAK1$^{LPC\text{-}KO}$/RIP3$^{-/-}$ [n = 6] and Ki67 staining: WT [n = 5]; TAK1$^{LPC\text{-}KO}$ [n = 8]; TAK1/Casp-8$^{LPC\text{-}KO}$ [n = 5]; TAK1$^{LPC\text{-}KO}$/RIP3$^{-/-}$ [n = 5]). The asterisk denotes $p < 0.05$, double asterisks denote $p < 0.01$, and triple asterisks denote $p < 0.001$.

(C) Western blot analysis of whole liver protein extracts from 6-week-old male TAK1$^{LPC\text{-}KO}$, TAK1/Casp-8$^{LPC\text{-}KO}$, TAK1$^{LPC\text{-}KO}$/RIP3$^{-/-}$, and control littermate mice (WT) using antibodies against PCNA, CycD1, cl. Casp-3, and GAPDH as loading control.

(D) Double stainings of pancytokeratin with Ki67 (upper panel; pancytokeratin is stained pink, Ki67 is stained brown) or cl. Casp-3 (lower panel; pancytokeratin is stained pink, cl. Casp-3 is stained brown). Arrowheads indicate double-stained cells.

(E) Statistical analysis of double-stained pancytokeratin^{+} and Ki67^{+} biliary epithelial cells in the respective 6-week-old mice. Results are shown as mean (n = 5); *$p < 0.05$; n.s., not significant.

(F) Statistical analysis of double-stained pancytokeratin^{+} and cl. Casp-3^{+} biliary epithelial cells in the respective 6-week-old mice. Results are shown as mean (n = 5). Double asterisks denote $p < 0.01$.

See also Figures S1 and S2.

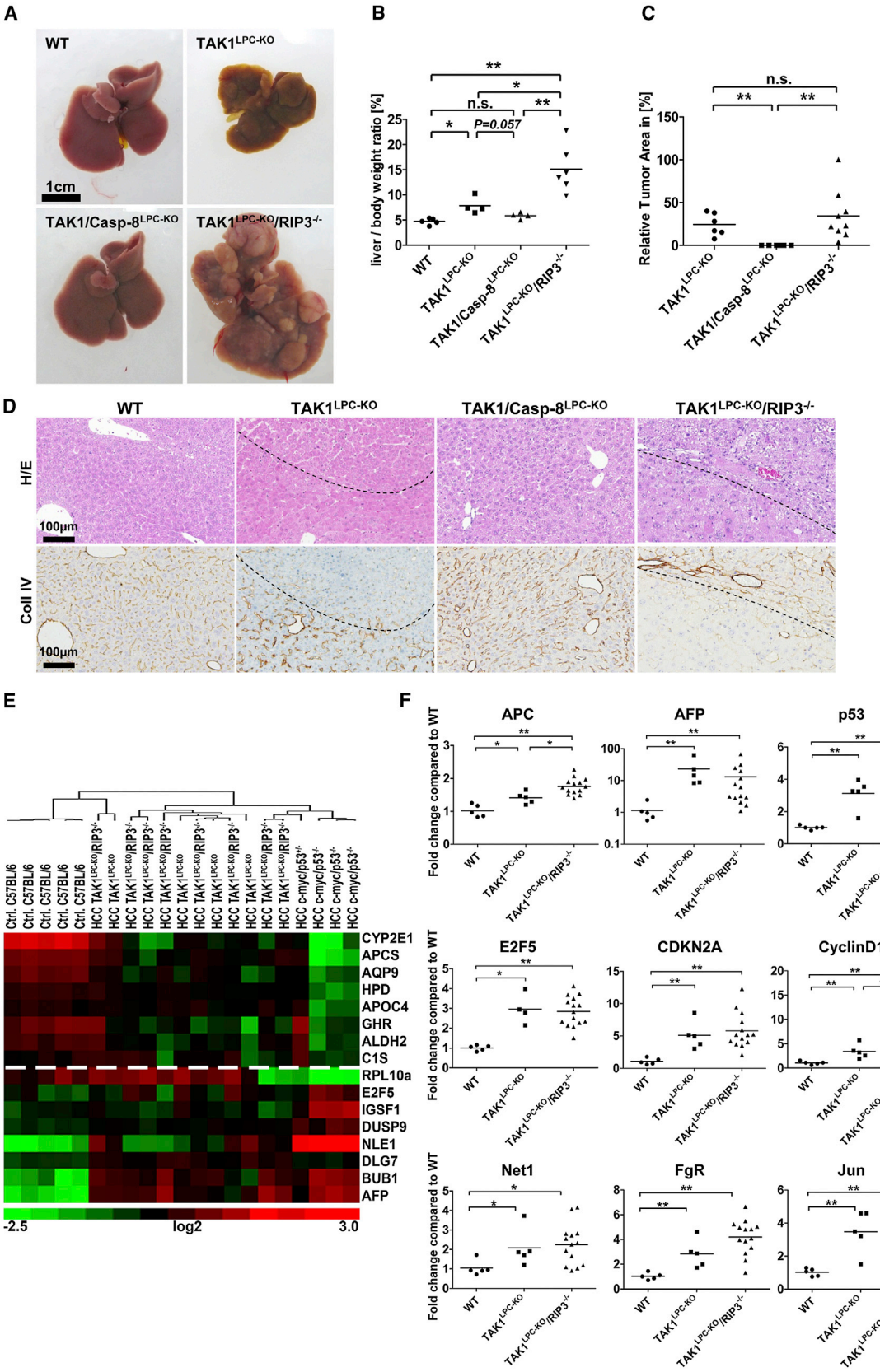

(legend on next page)

(Luedde and Schwabe, 2011)—are therefore extremely sensitive to LPS/TNF-induced liver failure and LPC apoptosis (Bettermann et al., 2010). However, we show that, already in livers of young TAK1^{LPC-KO}/RIP3$^{-/-}$ mice, a fraction of hepatocytes gained resistance toward TNF-dependent apoptosis, despite the absence of *Tak1*, and showed a pattern of chromosomal aberrations that was later found in HCC from these mice. These findings indicate that the specific chromosomal aberration pattern on chromosomes 4, 8, and 13 is not particularly acquired in late stages of tumor promotion but represents a fundamental genetic event involved in the earliest steps of tumor initiation in chronic inflammation in TAK1^{LPC-KO} mice. The exact nature of these genetic abnormalities is currently not clear, but they might lead to resistance toward apoptosis through the amplification of antiapoptotic genes or defective transcription of genes driving apoptosis in *Tak1*-deficient cells. Thus, further cytogenetic or transcriptomic analysis of TAK1^{LPC-KO}-HCCs might reveal novel candidate molecules or micro-RNAs involved in the regulation of apoptosis in *Tak1*-deficient cells. In addition, these findings might shed new light on the enigmatic processes of how chronic inflammation leads to genetic alterations in human patients with chronic liver disease.

In original definitions of apoptosis detected, for example, during organ development, intracellular contents are not released, and a consequent inflammatory response fails to develop, whereas the typical oncotic necrosis induced, for example, by ischemia is associated with release of cellular contents, initiating an inflammatory response (Jaeschke and Lemasters, 2003). By our genetic approach, we demonstrated that LPC apoptosis occurring in a pathological condition represents a much stronger trigger for inflammation and subsequent liver fibrosis than necroptosis. Given the concordant regulations between inflammation and fibrosis in TAK1^{LPC-KO}/RIP3$^{-/-}$ versus TAK1/Casp-8^{LPC-KO} livers, further comparative analyses in serum and cell culture supernatants between these two mouse models might allow the identification of novel paracrine factors linking apoptotic cell death of LPC with immune activation and hepatic fibrosis. Moreover, our data show that apoptosis and necroptosis have a fundamentally opposing function in regulating compensatory cell proliferation of surrounding cells in vivo. Whereas Caspase-8-dependent apoptosis in TAK1^{LPC-KO}/RIP3$^{-/-}$ mice led to a strong biliary reaction and expansion of bile ducts and oval cells in young animals, the "hyporegenerative" nature of necroptosis resulted in a disturbed biliary homeostasis and cholestasis. Interestingly, the intrahepatic number of bile ducts was significantly lower in TAK1^{LPC-KO} livers with combined presence of apoptosis and necroptosis than in TAK1/Casp-8^{LPC-KO} mice showing only necroptosis. This indicates that the complex biliary architecture might be even more sensitive to the onset of necroptosis in a setting with constant massive hepatocyte regeneration when apoptosis is simultaneously present. Whereas the mechanisms and functional implications of biliary ductular reactions are presently not well understood, the TAK1 model might shed new light on these processes and on paracrine mediators, linking cell death with differentiation and proliferation of bile duct cells.

Our data suggest that the MAP kinase JNK plays a critical role in the mediation of compensatory LPC proliferation in response to apoptosis. The function of JNK in liver cancer development was previously studied mainly in the model of diethylnitrosamine-dependent hepatocarcinogenesis, resulting in conflicting results with regards to a tumor promoting versus a tumor suppressive function in hepatocytes (Das et al., 2011; Sakurai et al., 2006). However, the proregenerative and presumably procarcinogenic function of JNK suggested by our data might depend on the presence of chronic inflammation preceding malignant transformation of hepatocytes, a situation present in most patients developing liver cancer (Llovet et al., 2003; Vucur et al., 2010). Moreover, our findings suggest that JNK not only acts upstream of Caspase-8 to control apoptosis, as previously shown (Chang et al., 2006), but is also regulated in response to Caspase-8, because ablation of Caspase-8 significantly dampened JNK activation in *Tak1*-deficient livers. Whether Caspase-8 controls JNK activation by cell-intrinsic signals (e.g., alternative MAP-3 kinases and their interaction with TNF receptor-associated factor or RIP modules [Karin and Gallagher, 2009]), or by cell-extrinsic mechanisms is presently unclear. Again, it is possible that, during carcinogenesis, certain genetic aberrations resulting in a condition similar to "undead cells" might promote JNK-dependent proliferation in response to apoptosis, a concept previously suggested in

Figure 4. Apoptosis Promotes Hepatocarcinogenesis, whereas Necroptosis Inhibits Cancer Growth in Livers of TAK1^{LPC-KO} Mice

(A) Representative macroscopic pictures of 33- to 35-week-old male WT (from left to the right), TAK1^{LPC-KO}, TAK1/Casp-8^{LPC-KO}, and TAK1^{LPC-KO}/RIP3$^{-/-}$ livers. The scale bars represent 1 cm.

(B) Body-weight ratio of 25- to 38-week-old male WT (n = 6), TAK1^{LPC-KO} (n = 4), TAK1/Casp-8^{LPC-KO} (n = 4), and TAK1^{LPC-KO}/RIP3$^{-/-}$ (n = 6) mice. The asterisk denotes $p < 0.05$ and double asterisks denote $p < 0.01$.

(C) Evaluation of tumor areas from H&E staining. TAK1^{LPC-KO} (n = 6), TAK1/Casp-8^{LPC-KO} (n = 6), and TAK1^{LPC-KO}/RIP3$^{-/-}$ (n = 9) livers. Results are shown as mean. Double asterisks denote $p < 0.01$.

(D) Representative slides from livers of a 28-week-old WT, TAK1^{LPC-KO}, TAK1/Casp-8^{LPC-KO}, and TAK1^{LPC-KO}/RIP3$^{-/-}$ mouse stained with H&E and collagen IV. Tumor borders are indicated by a dashed line.

(E) Sixteen gene profile analysis (heat map) of HCC derived from TAK1^{LPC-KO} and TAK1^{LPC-KO}/RIP3$^{-/-}$ livers (25- to 38-week-old mice). HCC were compared to aggressive liver tumors from WHV/N-myc2 p53^{+}/delta mice and control WT mice. Below the dashed line, genes indicating a proliferative phenotype are listed, whereas genes above the dashed white line represent a less proliferative, more differentiated phenotype. HCC derived from TAK1^{LPC-KO} and TAK1^{LPC-KO}/RIP3$^{-/-}$ livers show a similar proliferating phenotype.

(F) Relative (rel.) messenger RNA (mRNA) expression of the indicated oncogenes/tumor suppressor genes (APC, AFP, tumor protein p53 [p53], E2F5, CDKN2A, cyclin D1, Net1, Gardner-Rasheed feline sarcoma viral oncogene homolog [FgR], Jun oncogene [Jun]) of HCC derived from 25- to 38-week-old TAK1^{LPC-KO} (n = 5) and TAK1^{LPC-KO}/RIP3$^{-/-}$ (n = 14) mice as well as normal tissue from littermate control (WT) (n = 5). The asterisk denotes $p < 0.05$ and double asterisks denote $p < 0.01$.

See also Figure S2.

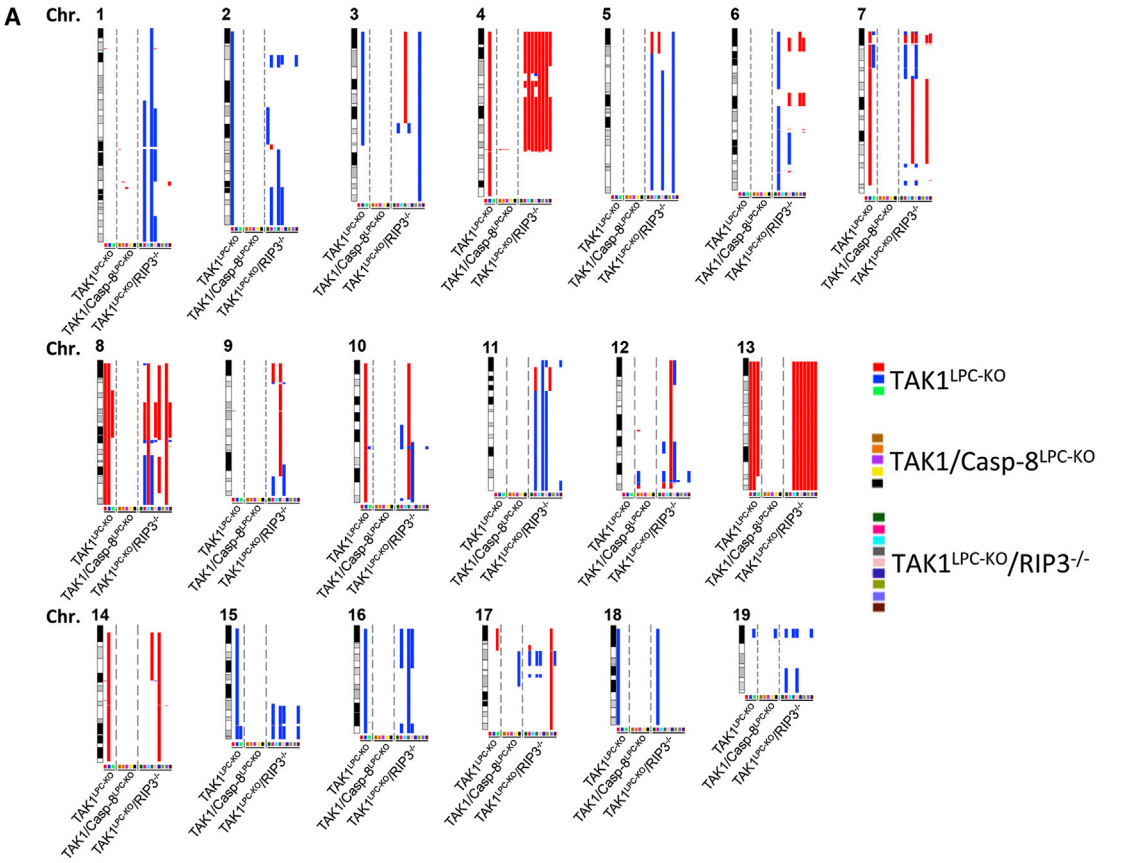

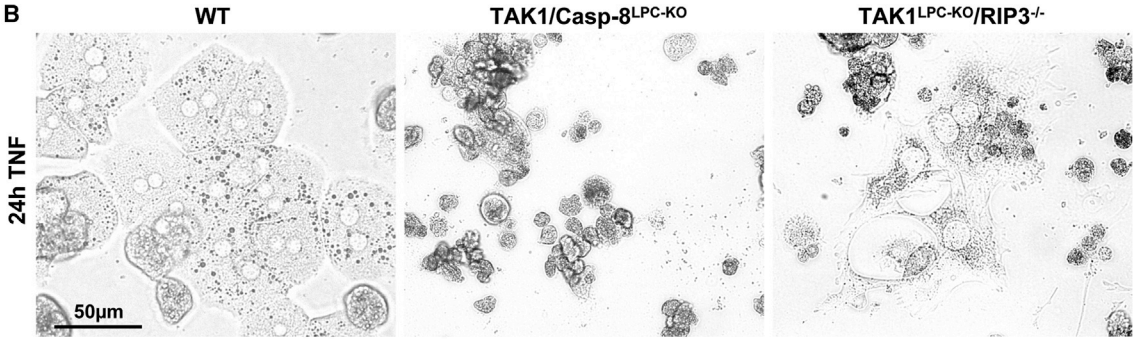

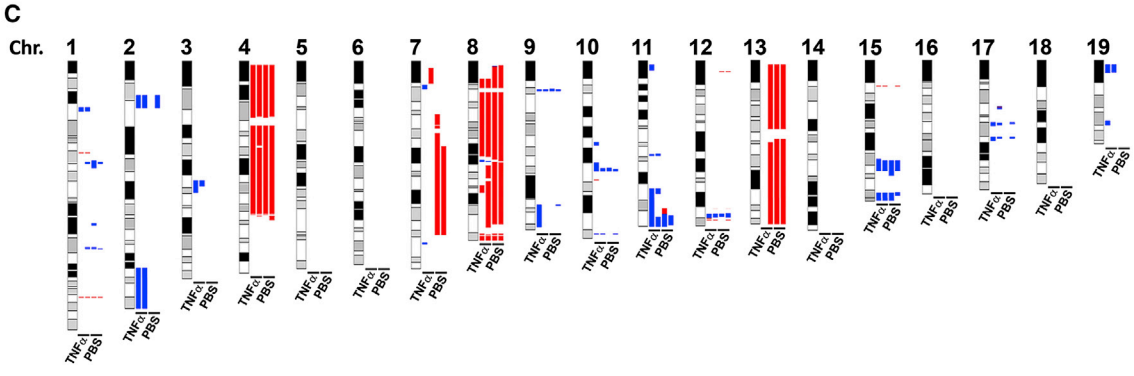

(legend on next page)

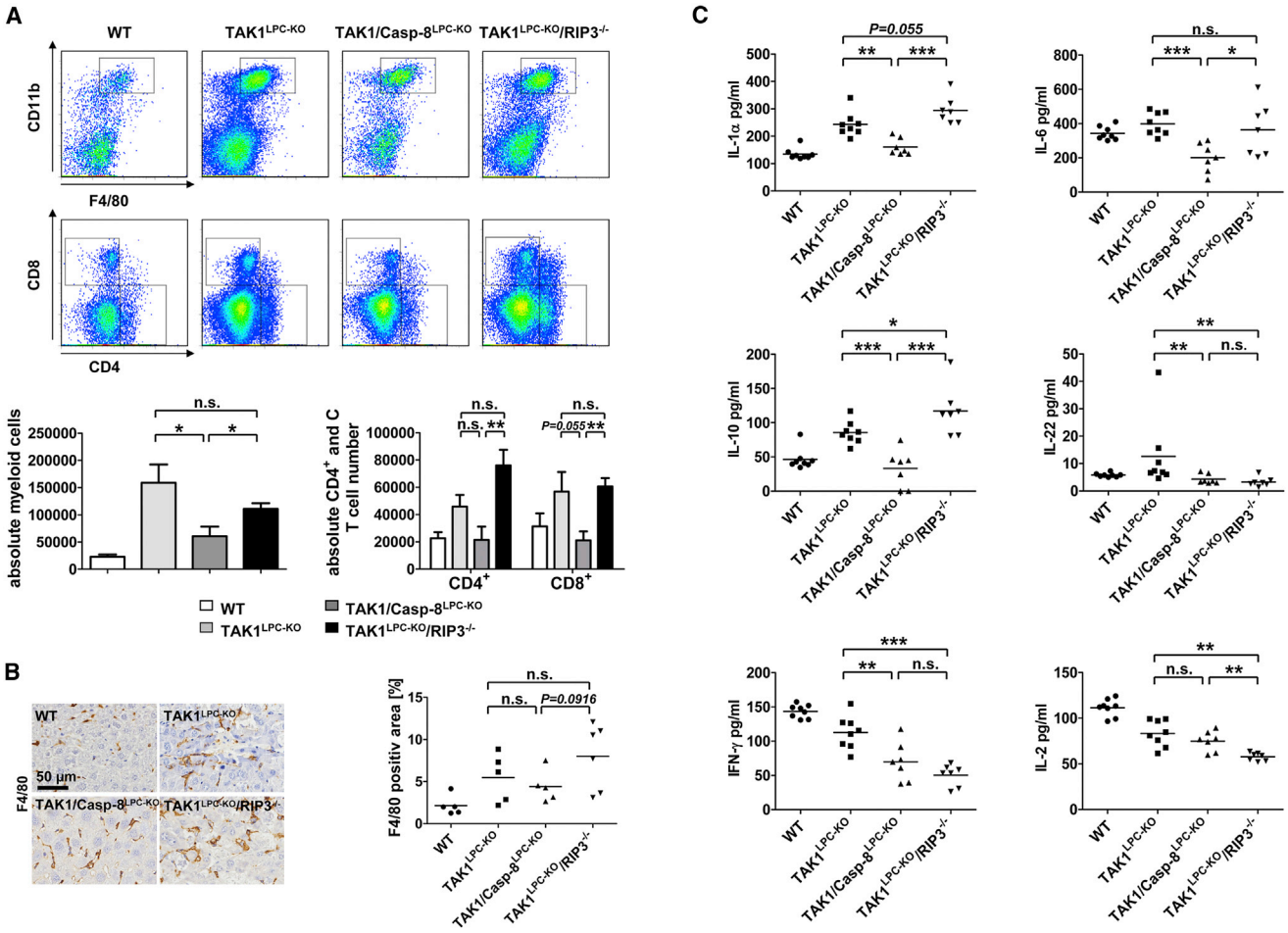

Figure 6. Differential Inductions of Inflammatory Responses by Apoptosis and Necroptosis in *Tak1*-Deficient Livers

(A) FACS-based analysis of infiltrating myeloid cells and T cells into liver tissue of TAK1^{LPC-KO}, TAK1/Casp-8^{LPC-KO}, and TAK1^{LPC-KO}/RIP3$^{-/-}$ mice. Results are shown as mean; error bars indicate SEM n = 5; *p < 0.05, **p < 0.01.

(B) Immunohistochemistry of liver paraffin sections and densitometric analysis for F4/80 in TAK1^{LPC-KO}, TAK1/Casp-8^{LPC-KO}, TAK1^{LPC-KO}/RIP3$^{-/-}$, and WT livers. Results are shown as mean; n = 5 for WT and TAK1/Casp-8^{LPC-KO}; n = 6 for TAK1^{LPC-KO}/RIP3$^{-/-}$. The scale bar represents 50 μm.

(C) FACS-based microbeads fluorescence assay for cytokine expression in liver protein homogenates. Results are shown as mean. n = 8 for WT and TAK1^{LPC-KO} and n = 7 for TAK1/Casp-8^{LPC-KO} and TAK1^{LPC-KO}/RIP3$^{-/-}$; *p < 0.05, **p < 0.01, ***p < 0.001.

See also Figure S4.

Drosophila (Ryoo and Bergmann, 2012). Interestingly, JNK activation was strongly increased in LPC (28-fold increase compared to WT) and less pronounced in NPC of TAK1^{LPC-KO}/RIP3$^{-/-}$ mice (1.18-fold increase compared to WT), favoring a parenchymal function of JNK. Moreover, it is presently unclear which specific factors released by apoptotic but not necroptotic parenchymal cells are involved in the activation process of immune cells, induction of chromosomal aberrations, and HCC development, but these processes might involve damage-associated molecular patterns/alarmins, such as high-mobility group protein 1, HMGN1, HSP60/HSP70, or β-defensins (Chan et al., 2012).

Figure 5. RIP3 Controls the Transition from Inflammation to Cancer by Inhibiting Chromosomal Aberrations Associated with Resistance of Hepatocytes toward Caspase-8-Dependent Apoptosis

(A) Summary of CGH analysis from three different hepatic tumors of three TAK1^{LPC-KO} mice, nine different tumors of nine TAK1^{LPC-KO}/RIP3$^{-/-}$ mice, and five samples of areas with disturbed histological architecture (no obvious tumors) from five TAK1/Casp-8^{LPC-KO} mice. The q-arm of each chromosome is shown and chromosome numbers are indicated. Dark horizontal bars within the symbolized chromosomes represent G bands. Chromosomal deletions are indicated in blue and amplifications in red. Individual mice are labeled by horizontal collared bars.

(B) Microscopic pictures of TNF-α-treated primary hepatocytes from WT, TAK1/Casp-8^{LPC-KO}, and TAK1^{LPC-KO}/RIP3$^{-/-}$ mice.

(C) Summary of CGH analysis from untreated and survived TNF-α-treated primary hepatocytes from TAK1^{LPC-KO}/RIP3$^{-/-}$ mice. Chromosomal amplifications and deletions are indicated in red and blue, respectively. IFN, interferon.

See also Figure S3.

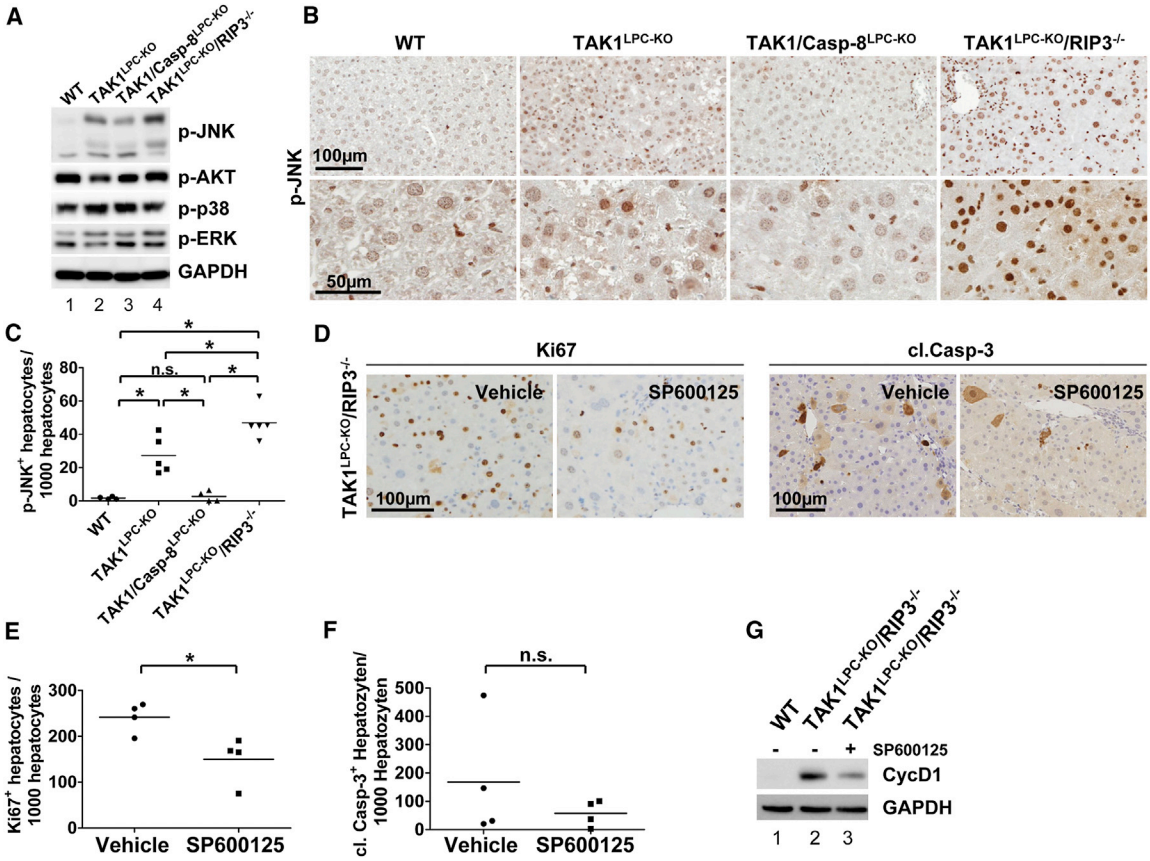

Figure 7. RIP3 Limits Compensatory Cell Proliferation through Inhibition of Caspase-8-Dependent JNK Activation

(A) Western blot analysis of whole liver-protein extracts from 6-week-old male TAK1^{LPC-KO}, TAK1/Casp-8^{LPC-KO}, TAK1^{LPC-KO}/RIP3$^{-/-}$, and control littermate mice (WT) using antibodies against the phosphorylated and active form of JNK, AKT, p38, ERK, and GAPDH as loading control.

(B) Immunohistochemistry of representative liver paraffin sections for phospho-JNK in 6-week-old mice. The scale bars represent 100 μm and 50 μm.

(C) Statistical analysis of p-JNK^{+} hepatocytes. Results are shown as mean. WT (n = 4), TAK1^{LPC-KO} (n = 5), TAK1/Casp-8^{LPC-KO} (n = 4), and TAK1^{LPC-KO}/RIP3$^{-/-}$ (n = 5) mice; *p < 0.0.

(D) Representative immunohistochemical analysis for Ki67 and cl. Casp-3 in 6-week-old mice treated with the JNK inhibitor SP600125 or vehicle as control.

(E) Statistical analysis of Ki67^{+} hepatocytes in animals treated with SP600125 compared to vehicle control-treated animals. Results are shown as mean. (n = 4); *p < 0.05.

(F) Statistical analysis of cl. Casp-3^{+} hepatocytes in TAK1^{LPC-KO}/RIP3$^{-/-}$ treated with SP600125 compared to vehicle control-treated mice. Results are shown as mean. (n = 4).

(G) Western blot analysis of whole liver protein extracts from 6-week-old male TAK1^{LPC-KO}/RIP3$^{-/-}$ and WT mice treated with SP600125 or vehicle using antibodies against CycD1 and GAPDH as loading control.

See also Figure S5.

Our findings indicate that mechanisms regulating the balance between necroptosis and apoptosis might be of great relevance for human liver disease and are in line with the clinical observation that an overbalance of necrotic over apoptotic hepatic cell death in acute liver failure is associated with a decreased regenerative capacity of the liver as a basis for a worse outcome (Bantel and Schulze-Osthoff, 2012). In addition, RIP3 mediates ethanol-induced liver injury (Roychowdhury et al., 2013). Thus, inhibition of RIP3-dependent or independent necrotic signaling pathways by novel molecular inhibitors might represent a promising approach in these settings. In addition, our findings indicate that LPC apoptosis plays a dominant role for the progression of chronic liver injury to liver cancer. Therefore, molecular inhibitors of caspases recently studied in patients with chronic hepatitis C virus infection (Pockros et al., 2007) or nonalcoholic steatohepatitis (Ratziu et al., 2012) might be especially useful in preventing the transition from chronic inflammation to hepatocarcinogenesis. Finally, inflammation is not only driving hepatocarcinogenesis but also the development of, for example, cancer of the colon (Greten et al., 2004), pancreas (Guerra et al., 2007), lung (Takahashi et al., 2010), or skin (Andreu et al., 2010). Hence, further studies in other cellular systems and organs are needed to examine if the paradigmatic functions of RIP3 versus Caspase-8 in regulating cellular compensatory proliferation and tumor growth in the liver represent a general principle in the control of epithelial cell homeostasis and cancer development.

EXPERIMENTAL PROCEDURES

Generation of Conditional Knockout Mice and Animal Experiments

Mice carrying loxP-site-flanked (floxed) alleles of the *Tak1* gene *Map3k7* (Tak1^{fl}) (Sato et al., 2005) or *Caspase-8* (Caspase-8^{fl}) (Salmena et al., 2003) were crossed to *Alfp*-Cre transgenic mice (Kellendonk et al., 2000) to generate a LPC-specific knockout of the respective genes (TAK1$^{LPC\text{-}KO}$, Caspase-8$^{LPC\text{-}KO}$). Mice with constitutive deletion of RIP3 (RIP3$^{-/-}$) were described before (Newton et al., 2004). Mice with combined conditional knockouts of *Map3k7* and constitutive ablation of *Rip3* (TAK1$^{LPC\text{-}KO}$/RIP3$^{-/-}$) as well as combined conditional ablations of *Map3k7* and *Caspase-8* (TAK1/Casp8$^{LPC\text{-}KO}$) as well as mice with constitutive ablations of *Rip3* and conditional ablations of *Map3k7* and *Caspase-8* in LPC (TAK1/Casp-8$^{LPC\text{-}KO}$/RIP3$^{-/-}$) were generated by intercrossing the respective lines. In all experiments, littermates carrying the respective loxP-flanked alleles but lacking expression of Cre recombinase were used as WT controls. Mice were bred on a mixed C57/BL6 - SV129Ola genetic background. Only sex-matched animals were compared. All animal experiments were approved by the Federal Ministry for Nature, Environment and Consumers' Protection of the state of North Rhine-Westphalia and were performed in accordance to the respective national, federal, and institutional regulations.

Surgery (partial hepatectomy) was performed on male mice of 6–8 weeks of age. Mice were anesthetized by isoflurane inhalation and treated with buprenorphine for analgesia. The abdominal cavity was opened by a midline laparotomy. The right median lobe, left median lobe, and left lateral lobe were identified and individually ligated. Mice were sacrificed at the indicated time points. Intraperitoneal injection of 15 μl SP600125 (1 mg/ABSOURCE) or vehicle (DMSO) was performed twice a day over 4 days on male mice of 5 weeks of age. Mice were sacrificed 3 hr after the last injection.

Statistics

Data were analyzed using PRISM software (GraphPad Software) and are expressed as mean. Statistical significance between experimental groups was assessed using an unpaired two-sample t test or Mann-Whitney test.

Further description of the Experimental Procedures is included within the Supplemental Information (Extended Experimental Procedures).

ACCESSION NUMBERS

The aCGH data have been deposited into the ArrayExpress database under accession number E-MTAB-1559 (http://www.ebi.ac.uk/arrayexpress/).

SUPPLEMENTAL INFORMATION

Supplemental Information includes Extended Experimental Procedures and five figures and can be found with this article online at http://dx.doi.org/10.1016/j.celrep.2013.07.035.

ACKNOWLEDGMENTS

The authors thank Dr. V. Dixit (Genentech, San Francisco, CA, USA) for kindly providing RIP3$^{-/-}$ mice, Dr. Shizuo Akira (Osaka, Japan) for kindly providing TAK1$^{fl/fl}$ mice, and Dr. Valentina M. Factor for kindly providing the A6 antibody. The authors are thankful for excellent technical support from Ruth Hillermann, Daniel Kull, and Olga Seelbach. T.L. was supported by the German Cancer Aid (Deutsche Krebshilfe 110043), an ERC Starting Grant (ERC-2007-Stg/208237-Luedde-Med3-Aachen), the German Research Foundation (SFB-TRR57/P06), the EMBO Young Investigator Program, the Interdisciplinary Centre for Clinical Research "BIOMAT" Aachen, the Ernst Jung Foundation Hamburg, and a grant from the medical faculty of the RWTH Aachen. M.H. was supported by the Helmholtz Foundation, the Hofschneider Foundation, the German Research Foundation (SFB-TR36), the Helmholtz Alliance Preclinical Comprehensive Center, and an ERC Starting Grant (LiverCancerMechanisms). M.L. was supported by the Deutsche Stiftung Herzforschung (12/12). This paper is dedicated to Dr. Uwe Walter Luedde (Bremerhaven/Germany) on the occasion of his 70th birthday.

Received: April 8, 2013
Revised: June 18, 2013
Accepted: July 26, 2013
Published: August 22, 2013

REFERENCES

Andreu, P., Johansson, M., Affara, N.I., Pucci, F., Tan, T., Junankar, S., Korets, L., Lam, J., Tawfik, D., DeNardo, D.G., et al. (2010). FcRgamma activation regulates inflammation-associated squamous carcinogenesis. Cancer Cell *17*, 121–134.

Bantel, H., and Schulze-Osthoff, K. (2012). Mechanisms of cell death in acute liver failure. Front. Physiol. *3*, 79.

Bettermann, K., Vucur, M., Haybaeck, J., Koppe, C., Janssen, J., Heymann, F., Weber, A., Weiskirchen, R., Liedtke, C., Gassler, N., et al. (2010). TAK1 suppresses a NEMO-dependent but NF-kappaB-independent pathway to liver cancer. Cancer Cell *17*, 481–496.

Bonnet, M.C., Preukschat, D., Welz, P.S., van Loo, G., Ermolaeva, M.A., Bloch, W., Haase, I., and Pasparakis, M. (2011). The adaptor protein FADD protects epidermal keratinocytes from necroptosis in vivo and prevents skin inflammation. Immunity *35*, 572–582.

Cairo, S., Armengol, C., De Reyniès, A., Wei, Y., Thomas, E., Renard, C.A., Goga, A., Balakrishnan, A., Semeraro, M., Gresh, L., et al. (2008). Hepatic stem-like phenotype and interplay of Wnt/beta-catenin and Myc signaling in aggressive childhood liver cancer. Cancer Cell *14*, 471–484.

Chakraborty, J.B., Oakley, F., and Walsh, M.J. (2012). Mechanisms and biomarkers of apoptosis in liver disease and fibrosis. Int. J. Hepatol. *2012*, 648915.

Chan, J.K., Roth, J., Oppenheim, J.J., Tracey, K.J., Vogl, T., Feldmann, M., Horwood, N., and Nanchahal, J. (2012). Alarmins: awaiting a clinical response. J. Clin. Invest. *122*, 2711–2719.

Chang, L., Kamata, H., Solinas, G., Luo, J.L., Maeda, S., Venuprasad, K., Liu, Y.C., and Karin, M. (2006). The E3 ubiquitin ligase itch couples JNK activation to TNFalpha-induced cell death by inducing c-FLIP(L) turnover. Cell *124*, 601–613.

Chen, L., Park, S.M., Tumanov, A.V., Hau, A., Sawada, K., Feig, C., Turner, J.R., Fu, Y.X., Romero, I.L., Lengyel, E., and Peter, M.E. (2010). CD95 promotes tumour growth. Nature *465*, 492–496.

Cho, Y.S., Challa, S., Moquin, D., Genga, R., Ray, T.D., Guildford, M., and Chan, F.K. (2009). Phosphorylation-driven assembly of the RIP1-RIP3 complex regulates programmed necrosis and virus-induced inflammation. Cell *137*, 1112–1123.

Das, M., Garlick, D.S., Greiner, D.L., and Davis, R.J. (2011). The role of JNK in the development of hepatocellular carcinoma. Genes Dev. *25*, 634–645.

Delaney, J.R., and Mlodzik, M. (2006). TGF-beta activated kinase-1: new insights into the diverse roles of TAK1 in development and immunity. Cell Cycle *5*, 2852–2855.

Desmet, V.J. (2011). Ductal plates in hepatic ductular reactions. Hypothesis and implications. I. Types of ductular reaction reconsidered. Virchows Arch. *458*, 251–259.

Dubois, C.M., Blanchette, F., Laprise, M.H., Leduc, R., Grondin, F., and Seidah, N.G. (2001). Evidence that furin is an authentic transforming growth factor-beta1-converting enzyme. Am. J. Pathol. *158*, 305–316.

Feldstein, A.E., and Gores, G.J. (2005). Apoptosis in alcoholic and nonalcoholic steatohepatitis. Front. Biosci. *10*, 3093–3099.

Fung, J., Lai, C.L., and Yuen, M.F. (2009). Hepatitis B and C virus-related carcinogenesis. Clin. Microbiol. Infect. *15*, 964–970.

Glaser, S.S., Gaudio, E., Miller, T., Alvaro, D., and Alpini, G. (2009). Cholangiocyte proliferation and liver fibrosis. Expert Rev. Mol. Med. *11*, e7.

Greten, F.R., Eckmann, L., Greten, T.F., Park, J.M., Li, Z.W., Egan, L.J., Kagnoff, M.F., and Karin, M. (2004). IKKbeta links inflammation and tumorigenesis in a mouse model of colitis-associated cancer. Cell *118*, 285–296.

Guerra, C., Schuhmacher, A.J., Cañamero, M., Grippo, P.J., Verdaguer, L., Pérez-Gallego, L., Dubus, P., Sandgren, E.P., and Barbacid, M. (2007). Chronic pancreatitis is essential for induction of pancreatic ductal adenocarcinoma by K-Ras oncogenes in adult mice. Cancer Cell *11*, 291–302.

Han, J., Zhong, C.Q., and Zhang, D.W. (2011). Programmed necrosis: backup to and competitor with apoptosis in the immune system. Nat. Immunol. *12*, 1143–1149.

Hanahan, D., and Weinberg, R.A. (2011). Hallmarks of cancer: the next generation. Cell *144*, 646–674.

He, S., Wang, L., Miao, L., Wang, T., Du, F., Zhao, L., and Wang, X. (2009). Receptor interacting protein kinase-3 determines cellular necrotic response to TNF-alpha. Cell *137*, 1100–1111.

Huh, J.R., Guo, M., and Hay, B.A. (2004). Compensatory proliferation induced by cell death in the Drosophila wing disc requires activity of the apical cell death caspase Dronc in a nonapoptotic role. Curr. Biol. *14*, 1262–1266.

Inokuchi, S., Aoyama, T., Miura, K., Osterreicher, C.H., Kodama, Y., Miyai, K., Akira, S., Brenner, D.A., and Seki, E. (2010). Disruption of TAK1 in hepatocytes causes hepatic injury, inflammation, fibrosis, and carcinogenesis. Proc. Natl. Acad. Sci. USA *107*, 844–849.

Jaeschke, H., and Lemasters, J.J. (2003). Apoptosis versus oncotic necrosis in hepatic ischemia/reperfusion injury. Gastroenterology *125*, 1246–1257.

Karin, M., and Gallagher, E. (2009). TNFR signaling: ubiquitin-conjugated TRAFfic signals control stop-and-go for MAPK signaling complexes. Immunol. Rev. *228*, 225–240.

Kellendonk, C., Opherk, C., Anlag, K., Schütz, G., and Tronche, F. (2000). Hepatocyte-specific expression of Cre recombinase. Genesis *26*, 151–153.

Kondo, S., Senoo-Matsuda, N., Hiromi, Y., and Miura, M. (2006). DRONC coordinates cell death and compensatory proliferation. Mol. Cell. Biol. *26*, 7258–7268.

Llovet, J.M., Burroughs, A., and Bruix, J. (2003). Hepatocellular carcinoma. Lancet *362*, 1907–1917.

Luedde, T., and Schwabe, R.F. (2011). NF-κB in the liver—linking injury, fibrosis and hepatocellular carcinoma. Nat. Rev. Gastroenterol. Hepatol. *8*, 108–118.

Luedde, T., Beraza, N., Kotsikoris, V., van Loo, G., Nenci, A., De Vos, R., Roskams, T., Trautwein, C., and Pasparakis, M. (2007). Deletion of NEMO/IKKgamma in liver parenchymal cells causes steatohepatitis and hepatocellular carcinoma. Cancer Cell *11*, 119–132.

Maeda, S., Kamata, H., Luo, J.L., Leffert, H., and Karin, M. (2005). IKKbeta couples hepatocyte death to cytokine-driven compensatory proliferation that promotes chemical hepatocarcinogenesis. Cell *121*, 977–990.

Michalopoulos, G.K., and DeFrances, M. (2005). Liver regeneration. Adv. Biochem. Eng. Biotechnol. *93*, 101–134.

Newton, K., Sun, X., and Dixit, V.M. (2004). Kinase RIP3 is dispensable for normal NF-kappa Bs, signaling by the B-cell and T-cell receptors, tumor necrosis factor receptor 1, and Toll-like receptors 2 and 4. Mol. Cell. Biol. *24*, 1464–1469.

Pockros, P.J., Schiff, E.R., Shiffman, M.L., McHutchison, J.G., Gish, R.G., Afdhal, N.H., Makhviladze, M., Huyghe, M., Hecht, D., Oltersdorf, T., and Shapiro, D.A. (2007). Oral IDN-6556, an antiapoptotic caspase inhibitor, may lower aminotransferase activity in patients with chronic hepatitis C. Hepatology *46*, 324–329.

Ratziu, V., Sheikh, M.Y., Sanyal, A.J., Lim, J.K., Conjeevaram, H., Chalasani, N., Abdelmalek, M., Bakken, A., Renou, C., Palmer, M., et al. (2012). A phase 2, randomized, double-blind, placebo-controlled study of GS-9450 in subjects with nonalcoholic steatohepatitis. Hepatology *55*, 419–428.

Renard, C.A., Fourel, G., Bralet, M.P., Degott, C., De La Coste, A., Perret, C., Tiollais, P., and Buendia, M.A. (2000). Hepatocellular carcinoma in WHV/N-myc2 transgenic mice: oncogenic mutations of beta-catenin and synergistic effect of p53 null alleles. Oncogene *19*, 2678–2686.

Roychowdhury, S., McMullen, M.R., Pisano, S.G., Liu, X., and Nagy, L.E. (2013). Absence of receptor interacting protein kinase 3 prevents ethanol-induced liver injury. Hepatology *57*, 1773–1783.

Ryoo, H.D., and Bergmann, A. (2012). The role of apoptosis-induced proliferation for regeneration and cancer. Cold Spring Harb. Perspect. Biol. *4*, a008797. http://dx.doi.org/10.1101/cshperspect.a008797.

Sakurai, T., Maeda, S., Chang, L., and Karin, M. (2006). Loss of hepatic NF-kappa B activity enhances chemical hepatocarcinogenesis through sustained c-Jun N-terminal kinase 1 activation. Proc. Natl. Acad. Sci. USA *103*, 10544–10551.

Sakurai, T., He, G., Matsuzawa, A., Yu, G.Y., Maeda, S., Hardiman, G., and Karin, M. (2008). Hepatocyte necrosis induced by oxidative stress and IL-1 alpha release mediate carcinogen-induced compensatory proliferation and liver tumorigenesis. Cancer Cell *14*, 156–165.

Salmena, L., Lemmers, B., Hakem, A., Matysiak-Zablocki, E., Murakami, K., Au, P.Y., Berry, D.M., Tamblyn, L., Shehabeldin, A., Migon, E., et al. (2003). Essential role for caspase 8 in T-cell homeostasis and T-cell-mediated immunity. Genes Dev. *17*, 883–895.

Sato, S., Sanjo, H., Takeda, K., Ninomiya-Tsuji, J., Yamamoto, M., Kawai, T., Matsumoto, K., Takeuchi, O., and Akira, S. (2005). Essential function for the kinase TAK1 in innate and adaptive immune responses. Nat. Immunol. *6*, 1087–1095.

Sherman, M. (2010). Hepatocellular carcinoma: epidemiology, surveillance, and diagnosis. Semin. Liver Dis. *30*, 3–16.

Takahashi, H., Ogata, H., Nishigaki, R., Broide, D.H., and Karin, M. (2010). Tobacco smoke promotes lung tumorigenesis by triggering IKKbeta- and JNK1-dependent inflammation. Cancer Cell *17*, 89–97.

Vanlangenakker, N., Vanden Berghe, T., Bogaert, P., Laukens, B., Zobel, K., Deshayes, K., Vucic, D., Fulda, S., Vandenabeele, P., and Bertrand, M.J. (2011). cIAP1 and TAK1 protect cells from TNF-induced necrosis by preventing RIP1/RIP3-dependent reactive oxygen species production. Cell Death Differ. *18*, 656–665.

Vucur, M., Roderburg, C., Bettermann, K., Tacke, F., Heikenwalder, M., Trautwein, C., and Luedde, T. (2010). Mouse models of hepatocarcinogenesis: what can we learn for the prevention of human hepatocellular carcinoma? Oncotarget *1*, 373–378.

Welz, P.S., Wullaert, A., Vlantis, K., Kondylis, V., Fernández-Majada, V., Ermolaeva, M., Kirsch, P., Sterner-Kock, A., van Loo, G., and Pasparakis, M. (2011). FADD prevents RIP3-mediated epithelial cell necrosis and chronic intestinal inflammation. Nature *477*, 330–334.

Wunderlich, F.T., Luedde, T., Singer, S., Schmidt-Supprian, M., Baumgartl, J., Schirmacher, P., Pasparakis, M., and Brüning, J.C. (2008). Hepatic NF-kappa B essential modulator deficiency prevents obesity-induced insulin resistance but synergizes with high-fat feeding in tumorigenesis. Proc. Natl. Acad. Sci. USA *105*, 1297–1302.

Yang, L., Inokuchi, S., Roh, Y.S., Song, J., Loomba, R., Park, E.J., and Seki, E. (2013). Transforming growth factor-β signaling in hepatocytes promotes hepatic fibrosis and carcinogenesis in mice with hepatocyte-specific deletion of TAK1. Gastroenterology *144*, 1042–1054.e4.

Zhang, D.Y., and Friedman, S.L. (2012). Fibrosis-dependent mechanisms of hepatocarcinogenesis. Hepatology *56*, 769–775.

Zhang, D.W., Shao, J., Lin, J., Zhang, N., Lu, B.J., Lin, S.C., Dong, M.Q., and Han, J. (2009). RIP3, an energy metabolism regulator that switches TNF-induced cell death from apoptosis to necrosis. Science *325*, 332–336.